Dalton Transactions

ROYAL SOCIETY OF CHEMISTRY

PAPER

View Article Online
View Journal

Open Access Article. Published on 26 February 2026. Downloaded on 3/19/2026 8:38:46 PM.
This article is licensed under a Creative Commons Attribution 3.0 Unported Licence.

Check for updates

Cite this: DOI: 10.1039/d6dt00234j

Accessing osmium(VI) nitrido complexes with N-heterocyclic carbene ligands

Joshua Parche, Robin Sievers, Tim-Niclas Streit and Moritz Malischewski *

Received 29th January 2026,
Accepted 24th February 2026

DOI: 10.1039/d6dt00234j

rsc.li/dalton

The synthesis of the first osmium(VI) nitrido complexes bearing NHC ligands is described. Herein, $[NBu_4][OsNCl_4]$ is reacted with two equivalents of Cl-IMes NHC to afford the neutral complex $[OsN(Cl)_3(Cl\text{-}IMes)_2]$. Subsequent ligand substitution reactions selectively replace the chloride ligands while preserving the OsN–NHC core, providing access to a series of stable complexes of the general formula $[OsN(X)_3(Cl\text{-}IMes)_2]$. These compounds represent the first examples of osmium–NHC complexes in an oxidation state higher than +IV. The ligand exchange reactions enable systematic tuning of the coordination environment and the associated electronic properties.

Introduction

The isolation of the first stable carbene – an N-heterocyclic carbene (NHC) – by Arduengo and co-workers in 1991 marked a turning point in modern chemistry.[1] The remarkable stability of this imidazolylidene carbene arises from the electronic contributions of the adjacent nitrogen atoms as well as from sterically demanding substituents that suppress carbene dimerization.[2,3] Since this seminal discovery, a wide variety of NHCs has been developed, enabling numerous applications in catalysis and coordination chemistry.[2,4] Although often compared to tertiary phosphines as neutral two-electron donor ligands, NHCs offer enhanced σ-donor strength, which reduces their tendency to dissociate from metal centers. This feature has stimulated extensive research into NHC transition–metal complexes. Moreover, the ability to independently tune the steric and electronic properties of NHCs provides a powerful means of optimizing catalytic performance.[2,5] Many NHC-based catalysts now surpass their phosphine analogues in both activity and stability, while also tolerating a broader range of reaction conditions.[6–12]

The strong σ-donor character of N-heterocyclic carbenes has further enabled the stabilization of transition–metal complexes in high oxidation states. Although free carbenes are generally prone to oxidation, they become remarkably robust upon coordination to a metal center, in contrast to phosphines, which are rarely employed under strongly oxidizing conditions due to their limited oxidative stability.[10,13] For instance, CH_3ReO_3 (MTO), an organometallic complex of rhenium in its highest oxidation state that functions as both a stoichiometric and catalytic oxidant, forms a stable adduct with an NHC without leading to its oxidation.[10,13] Since this report, several high-valent NHC complexes have been described bearing oxo and nitrido ligands, such as the first cationic Mo(VI) complexes,[14] stable oxo-vanadium(V) complexes,[15] and numerous Tc(V) and Re(V) nitrido complexes,[16] underscoring the effectiveness of NHCs in stabilizing high-oxidation-state metal centers. This capability has facilitated significant advances in catalysis by enabling the formation of robust metal–NHC complexes that tolerate strongly oxidizing conditions as well as highly oxidized metal centers.[3]

Although metal–NHC complexes have been reported for third-row transition metals, most notably for rhenium, the vast majority of studies have focused on NHC complexes of first- and second-row metals.[17] This trend is clear when comparing group 8 transition metals: numerous NHC complexes are known for iron and ruthenium, yet osmium analogues remain comparatively rare.[18–21] Despite the close structural similarity between osmium and ruthenium complexes, osmium species have often been overlooked because their higher kinetic inertness leads to their use primarily as stable models of reactive intermediates in catalytic cycles.[19,22] Nevertheless, osmium NHC complexes are now attracting growing interest as their unique and potentially valuable properties continue to emerge. These osmium NHC complexes find utility as building blocks for long-lived emissive complexes,[6,23] as key components in research focused on creating more effective metallodrugs[22] and as redox mediators.[24] Despite the proven ability of NHCs to stabilize high oxidation states and the inherent accessibility of high oxidation states in osmium complexes, the known osmium–NHC compounds are predominantly limited to the +II oxidation state, with only a few osmium(IV) examples reported to date (Fig. 1).[17–19,21,22,24–26] Furthermore, osmium(VI) nitrido complexes are of particular interest in

Freie Universität Berlin, Institute of Inorganic Chemistry, Fabeckstr. 34-36, 14195 Berlin, Germany. E-mail: moritz.malischewski@fu-berlin.de

Open Access Article. Published on 26 February 2026. Downloaded on 3/19/2026 8:38:46 PM.
This article is licensed under a Creative Commons Attribution 3.0 Unported Licence.

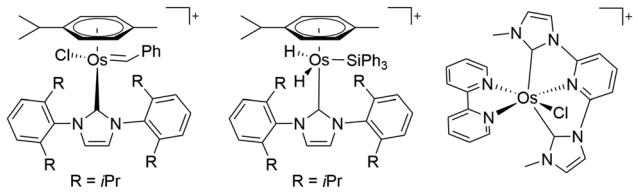

Fig. 1 Selected examples of osmium NHC complexes.[17,18,26]

photochemistry due to their distinctive absorption bands and long-lived excited states, which are essential for light-driven processes.[27–30] In this context, examining osmium(VI) nitrido complexes carrying NHC ligands could inspire further investigations in this field.

We report herein the synthesis of the first osmium nitrido complex bearing an NHC ligand, which, to the best of our knowledge, represents the first example of an osmium NHC complex in an oxidation state higher than +IV. Furthermore, we demonstrate the possibility of exchanging the chlorido ligands in the resulting complex by simple salt metathesis reactions.

Results and discussion

A likely reason why osmium(VI) nitrido complexes containing NHC ligands have not yet been reported is that nucleophiles tend to attack the nitrido ligand rather than coordinate to the metal center. Such reactivity has been observed in several cases, including reactions between Os(VI) nitrido complexes and carbene precursors. In these reactions, nucleophilic attack results in the formation of a C–N double bond between the carbene carbon and the nitrido ligand, accompanied by the reduction of the metal center to Os(IV).[31] Similar outcomes are observed when Os(VI) nitrido complexes are treated with PPh_3, yielding Os(V) or Os(IV) phosphoraniminato complexes (Scheme 1, top).[32,33]

In this work, we investigated the coordination of NHC ligands to the Os(VI) nitrido precursor $[NBu_4][OsNCl_4]$. A series of imidazolylidene- and imidazolinylidene-based carbenes, including SIMes and IMes, was examined; however, these reactions generally resulted in the formation of unidentifiable product mixtures containing varying amounts of the respective imidazolium salts. In contrast, the IMes-type NHC bearing a chlorinated backbone (Cl-IMes) could be successfully coordinated to the Os(VI) nitrido center. Slow addition of a THF solution containing two equivalents of Cl-IMes to a stirred solution of $[NBu_4][OsNCl_4]$ resulted, after overnight stirring, in the formation of a red solution. In contrast to analogous reactions with other NHCs, this process cleanly afforded the complex $[OsN(Cl)_3(Cl\text{-}IMes)_2]$ (**1**) in good yield (75%) (Scheme 1, bottom). The slow addition of the carbene is crucial to obtain complex **1** in good yields. Formation of **1** proceeds *via* substitution of one chlorido ligand to generate NBu_4Cl, which can be removed by filtration, yielding the OsN–NHC complex as a pure red solid (see the Experimental section). If present, any excess free NHC was removed by washing the solid with minimal amounts of pentane. The resulting complex, $[OsN(Cl)_3(Cl\text{-}IMes)_2]$ (**1**), exhibits high stability and may be stored indefinitely under an argon atmosphere, either in solution or in the solid state. It also shows limited stability upon exposure to air. However, complex **1** undergoes slow decomposition in C–H acidic solvents such as $CHCl_3$ and CH_2Cl_2 as well as in MeCN, ultimately leading to the formation of the corresponding Cl-IMes imidazolium salt, which can be detected by ^{1}H NMR spectroscopy, along with dark precipitates corresponding to osmium-containing decomposition products.

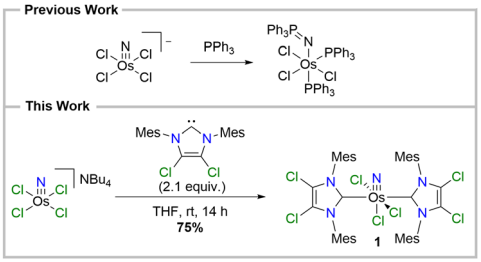

Scheme 1 Reactivity of $[OsNCl_4]^-$ with nucleophiles leading to reduced complexes[33] (top) or under the retention of the oxidation state (bottom).

The selective formation of **1** is attributed to the reduced σ-donor strength and enhanced π-acceptor character of Cl-IMes relative to non-halogenated IMes derivatives, as reflected in the reported Tolman electronic parameter trends for backbone-halogenated NHCs.[2,34] The reduced σ-donor strength of this carbene results in a less reactive carbene, which may react more selectively towards coordination to the Os(VI) nitrido center instead of attacking the nitrido ligand. In addition to moderating σ-donation, the increased π-accepting ability of Cl-IMes enables partial back-donation from the Os(VI) center to the carbene ligand, thereby stabilizing the Os–C_{NHC} bond in the presence of the strongly π-donating nitrido ligand. The electronic features matched well with the Os(VI) nitrido fragment, avoiding excessive electron donation that could otherwise destabilize the resulting metal complex.

The newly synthesized osmium(VI) NHC complex **1** is diamagnetic, which is consistent with osmium complexes in a d^2 configuration coordinated by π-donating ligands.[35] The ^{1}H NMR spectrum of complex **1** shows a single set of signals for both NHCs, as expected for magnetically equivalent ligands. The aromatic protons of the NHC exhibit a high field shift to 6.52 ppm relative to the free carbene (6.65 ppm), which likely arises due to π-backdonation from the metal center to the carbene ligands. In addition, splitting of the CH_3 signals is observed in complex **1**, giving two singlets at 2.24 and 2.05 ppm, assigned to the *ortho* and *para* substituents, respectively, while the free carbene displays a single broad resonance at 2.02 ppm corresponding to both substituents of the mesityl groups (see the SI). The ^{13}C NMR spectrum of complex **1** revealed a new signal at 157.9 ppm, likely corresponding to the carbene carbon, which is significantly high-field shifted com-

Open Access Article. Published on 26 February 2026. Downloaded on 3/19/2026 8:38:46 PM.
This article is licensed under a Creative Commons Attribution 3.0 Unported Licence.

pared with the free carbene, which exhibits a respective signal at 219.9 ppm, while the remaining signals appear at comparable shifts.[36] Furthermore, mass spectrometric analysis revealed the cationic fragment $[OsN(Cl)_2(Cl\text{-}IMes)_2]^+$ at m/z = 1022.1313, arising from the loss of Cl^-.

Single crystals suitable for X-ray diffraction (XRD) analysis of $[OsN(Cl)_3(Cl\text{-}IMes)_2]$ (**1**) were obtained as clear red blocks by slowly cooling a solution in CH_2Cl_2/*n*-pentane (1 : 1) to −70 °C. This was, however, prior to the observation that complex **1** slowly decomposes in CH_2Cl_2. Crystals may also be obtained by cooling a respective toluene solution to −70 °C. Complex **1** crystallizes in the monoclinic space group $P2_1/n$ with one molecule and three CH_2Cl_2 solvent molecules per unit cell and exhibits a pseudo-octahedral geometry (Fig. 2). However, a twist of 28.9° between the planes of the two NHC ligands is observed to avoid steric repulsion between the mesityl substituents (Fig. S14). The N–Os–C angles remain close to 90°, as expected for octahedral complexes. The N–Os–Cl angle for chlorido ligands *cis* to the nitrido ligand increases to 95.6°, while the Os–Cl bond *trans* to the nitrido is significantly elongated to 2.450(1) Å, compared to 2.376(1) Å for the *cis* ligands, reflecting the strong *trans* effect of the nitrido group. The Os–N bond length of 1.642(4) Å aligns with typical osmium–nitrogen triple bonds, observed in octahedral and square planar Os(VI) nitrido complexes (Table 1).[37,38]

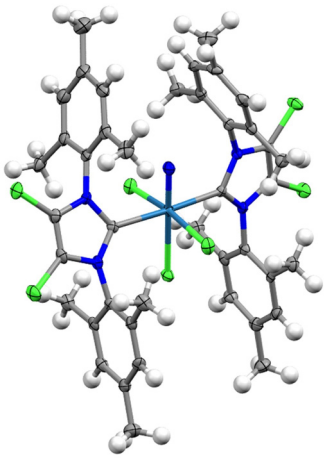

Fig. 2 Molecular structure of complex **1** in the solid state. Solvent molecules and disorders are omitted for clarity. Ellipsoids are depicted with a 50% probability level. Color code: light-blue, osmium; green, chlorine; blue, nitrogen; grey, carbon; and white, hydrogen.

Table 1 Selected bond lengths (Å) and angles (°) of complexes **1–4**. *Cis* and *trans* refer to the relative positions of the ligands with respect to the nitrido ligand

Complex	d(Os–N)	d(Os–C)	d(Os–X_{cis})	d(Os–X_{trans})	θ(N–Os–X_{cis})
1	1.642(4)	2.171(5)	2.376(1)	2.450(1)	98.0(2)
2	1.643(10)	2.158(7)	2.084(7)	2.094(8)	94.6(2)
3	1.730(8)	2.145(7)	2.377(2)	1.934(5)	95.18(5)
4	1.655(6)	2.109(9)	1.966(4)	1.958(5)	95.0(3)

Ligand exchange at complex **1** was investigated *via* salt metathesis with azide- and fluoride-containing salts. Treatment of **1** with excess NaN_3 in THF leads cleanly to threefold substitution of the chloride ligands, producing the triazido complex $[OsN(N_3)_3(Cl\text{-}IMes)_2]$ (**2**) in quantitative yield (Scheme 2, top). Attempts to introduce fluorido ligands revealed striking differences depending on the reagent. The reaction between KF and complex **1** produces a mixture of partially fluorinated species, tentatively assigned as $[OsN(Cl)_{3-x}(F)_x(Cl\text{-}IMes)_2]$. In contrast, by applying TlF as a salt, the selective replacement of the *trans* chlorido ligand was observed, yielding $[OsN(Cl)_2(F)(Cl\text{-}IMes)_2]$ (**3**) exclusively. Notably, AgF promotes complete replacement of all chlorido ligands, under otherwise identical conditions, forming the complex $[OsN(F)_3(Cl\text{-}IMes)_2]$ (**4**) in quantitative yield (Scheme 2, bottom). Interestingly, the choice of fluoride source proved critical: NaF is unreactive, while CsF induces the decomposition of **1**, highlighting the subtle interplay between the reagent and complex in controlling halide substitution. All three newly synthesized complexes **2–4** are highly stable under an argon atmosphere, comparable to complex **1**. The triazido complex **2** shows, as in complex **1**, limited stability in acidic solvents, leading to the protonation of the NHC ligands. In contrast, complexes **3** and **4** exhibit enhanced stability, showing no signs of decomposition after several days in CH_2Cl_2 solution.

In contrast to complex **1**, the osmium nitrido complexes **2** and **4** exhibit downfield-shifted aromatic proton resonances of the NHC ligands in their ^1H NMR spectra, appearing at 6.73 and 6.69 ppm, respectively, relative to the free carbene (6.65 ppm). By comparison, the corresponding signal for complex **3** is slightly high field shifted to 6.61 ppm. Notably, complex **4** displays inversion of the CH_3 resonances of the mesityl substituents, with the *para*-methyl signals appearing further downfield than those of the *ortho*-methyl groups (see the SI). Furthermore, ^{19}F NMR spectra reveal a singlet at −234.8 ppm for complex **3**, and a triplet at −214.6 ppm and a doublet at −337.2 ppm for complex **4**, consistent with the proposed structures depicted in Scheme 2. Acquisition of the ^{13}C NMR spectra of complexes **2–4** was attempted; however, owing

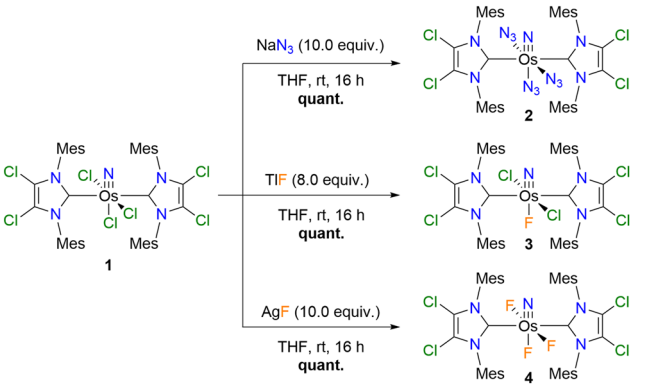

Scheme 2 Ligand exchange reactions of complex **1**.

Open Access Article. Published on 26 February 2026. Downloaded on 3/19/2026 8:38:46 PM.
This article is licensed under a Creative Commons Attribution 3.0 Unported Licence.

to their significantly reduced solubility compared to complex **1**, most resonances could not be observed, even at substantially increased numbers of scans. In addition, cationic fragments of complexes **2–4**, arising from the loss of one anionic ligand, were found by mass spectrometry, further confirming their structure (see the Experimental section).

Single crystals of $[OsN(N_3)_3(Cl\text{-}IMes)_2]$ (**2**) suitable for XRD analysis were obtained as clear red blocks by slowly cooling a THF solution to −70 °C. Complex **2** crystallizes in the monoclinic space group *C*2/*c*, with half of the molecule and two THF molecules present in the asymmetric unit (Fig. 3, left). The observed bond lengths and angles are comparable to those of complex **1**; however, a more pronounced twisting of the NHC ligands is evident, with an interplanar angle of 58.7° (Fig. S14). Furthermore, the bond lengths of the azido ligands in *cis* and *trans* positions relative to the nitrido ligand remain similar (Table 1). Notably, the *cis*-azido ligands display a bent coordination mode, whereas the *trans*-azido ligand adopts a linear coordination geometry. Single crystals of $[OsN(Cl)_2(F)(Cl\text{-}IMes)_2]$ (**3**) were obtained as clear yellow needles by slowly cooling a solution of THF/*n*-pentane (1 : 1) to −70 °C. Complex **3** crystallizes in the orthorhombic space group *Pcca*, with half of the molecule in the asymmetric unit (Fig. 3, middle). While most bond lengths and angles are comparable to those observed for complex **1**, a notable elongation of the Os–N bond to 1.730(8) Å is observed, although this value remains within the range reported for metal–nitrogen triple bonds.[32] In contrast, the Os–F bond *trans* to the nitrido ligand is relatively short, at 1.934(5) Å (Table 1). Single crystals of $[OsN(F)_3(Cl\text{-}IMes)_2]$ (**4**) were obtained as clear yellow needles by slowly cooling a solution of THF/*n*-pentane (1 : 1) to −70 °C. Complex **4** crystallizes in the monoclinic space group $P2_1/c$, with one molecule in the asymmetric unit, along with one molecule of *n*-pentane (Fig. 3, left). It should be noted that the diffraction data were solved at a relatively low resolution (2θ = 41.7°) due to crystal twinning, with a twin ratio of approximately 80 : 20. The structure was refined without explicitly treating the twin, as integration of the data as a twinned model resulted in a poorer solution. Nevertheless, the observed bond lengths and angles are largely comparable to those of complex **1**, with the exception of a significantly shortened Os–C bond of 2.109(9) Å. The shorter Os–C bonds in complexes **3** and **4** are in agreement with the enhanced stabilities of these complexes in acidic solvents.

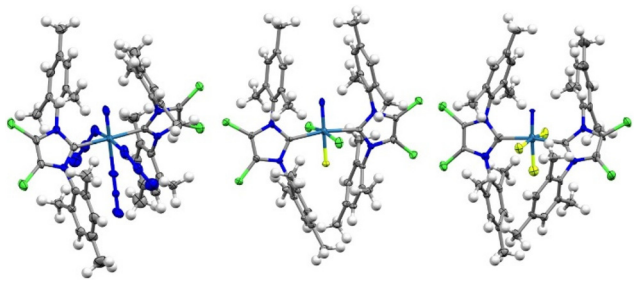

Fig. 3 Molecular structures of complexes **2** (left), **3** (middle) and **4** (right) in the solid state. Solvent molecules and disorders are omitted for clarity. Ellipsoids are depicted with a 50% probability level. Color code: light-blue, osmium; green, chlorine; yellow, fluorine; blue, nitrogen; grey, carbon; and white, hydrogen.

Table 2 Calculated Os–N vibrations of complexes **1–4** (B3LYP-D3BJ/def2svp). The respective frequencies were multiplied by a factor of 0.967

Complex	Os–N vibration
$[OsN(Cl)_3(Cl\text{-}IMes)_2]$ (**1**)	1084 cm^{-1}
$[OsN(N_3)_3(Cl\text{-}IMes)_2]$ (**2**)	1081 cm^{-1}
$[OsN(Cl)_2(F)(Cl\text{-}IMes)_2]$ (**3**)	1108 cm^{-1}
$[OsN(F)_3(Cl\text{-}IMes)_2]$ (**4**)	1104 cm^{-1}

Since the IR spectra of complexes **1–4** are mainly dominated by the NHC ligands, DFT calculations (B3LYP-D3BJ/def2svp) were performed to aid in the assignment of the Os–N stretching modes. As a reference, the IR frequencies of the anionic fragment $[OsNCl_4]^-$ were first calculated at the same level of theory, yielding an Os–N stretching frequency of 1200 cm^{-1}. Application of the literature-reported scaling factor of 0.967 for the chosen functional and basis set reduces this value to 1160 cm^{-1}, which is in improved agreement with the experimentally observed frequency of 1125 cm^{-1}.[39] Accordingly, the calculated Os–N stretching frequencies of complexes **1–4** were scaled by the same factor (Table 2). The resulting values correspond well to the intense and broad absorptions observed in the IR spectra of these complexes, indicating a slight weakening of the Os–N bond upon coordination of the NHC ligands. This effect is less pronounced for complexes **3** and **4**, which contain strongly electron-withdrawing F^- ligands. Overall, these observations suggest that complexes **1–4** are relatively electron rich, leading to weakening of the metal–nitrido bond, in agreement with the introduction of strongly σ-donating NHC ligands. In contrast, coordination of electron-withdrawing ligands generally results in a shift of the Os–N stretching vibration to higher frequencies, as observed in complexes bearing perfluorinated ligands.[37]

Conclusions

In conclusion, we have developed a straightforward method for synthesizing the first osmium(VI) nitrido complexes featuring NHC ligands. This approach enables coordination of two NHC ligands to the Os–N center of $[NBu_4][OsNCl_4]$, yielding the neutral complex $[OsN(Cl)_3(Cl\text{-}IMes)_2]$ (**1**). Subsequent ligand exchange reactions allow selective replacement of chlorido ligands without disrupting the OsN–NHC core, producing complexes of the general formula $[OsN(X)_3(Cl\text{-}IMes)_2]$. To the best of our knowledge, osmium NHC complexes in oxidation states above +IV have not been reported previously, highlighting the potential of these new complexes to exhibit unique electronic and structural properties. The simplicity of the ligand exchange strategy further provides a convenient means to fine-tune these properties *via* selective ligand modification.

Open Access Article. Published on 26 February 2026. Downloaded on 3/19/2026 8:38:46 PM.
This article is licensed under a Creative Commons Attribution 3.0 Unported Licence.

The resulting complexes are fully characterized and demonstrate remarkable stability.

Experimental section

Synthesis of $[NBu_4][OsNCl_4]$

The synthesis of $[NBu_4][OsNCl_4]$ was performed according to a procedure described by Griffith and Pawson.[40] $K_2[OsO_2(OH)_4]$ (0.8 g, 2.17 mmol, 1.0 equiv.) was placed in a 50 mL round-bottom flask and dissolved in 12 mL of concentrated HCl. A solution of NaN_3 (0.3 g, 4.78 mmol, 2.2 equiv.) in 4 mL of H_2O was added slowly to the solution and the reaction mixture was stirred at rt for 20 min. $[NBu_4]Cl$ (0.9 g, 3.26 mmol, 1.5 equiv.) was added as a solid, leading to the rapid formation of a pink precipitate. The precipitate was filtered off and washed with H_2O (20 mL) and Et_2O (20 mL) and dried under high vacuum to obtain $[NBu_4][OsNCl_4]$ (1.3 g, 2.17 mmol, **quant.**) as a pink solid.

FT-IR (ATR) ν [cm^{-1}]: 2962 (m), 2874 (m), 1468 (s), 1380 (w), 1320 (w), 1239 (w), 1168 (w), 1125 (m), 1068 (w), 1034 (w), 991 (w), 923 (w), 883 (m), 797 (w), 734 (m).

The analytical data are in agreement with the reported literature.[40]

Synthesis of Cl-IMes

The synthesis of Cl-IMes was performed according to a procedure described by Arduengo *et al.*[36] A 100 mL Schlenk flask was charged with IMes (2.00 g, 6.6 mmol, 1.0 equiv.) and 40 mL of degassed THF. To the resulting solution, degassed CCl_4 (1.27 mL, 13.1 mmol, 2.0 equiv.) in 10 mL of degassed THF was added slowly, and the reaction mixture was stirred at rt for 20 min. The volatiles were removed under high vacuum to obtain Cl-IMes (2.46 g, 6.6 mmol, **quant.**) as a yellow solid. If necessary, further purification may be accomplished by recrystallization from THF.

^{1}H NMR (401 MHz, C_6D_6, rt) δ [ppm] = 6.65 (s, 4H, H_{Ar}), 2.02 (s, 18H, H_{Bn}).

The analytical data are in agreement with the reported literature.[36]

Synthesis of $[OsN(Cl)_3(Cl\text{-}IMes)_2]$ (1)

$[NBu_4][OsNCl_4]$ (235 mg, 0.4 mmol, 1.0 equiv.) was placed in a 50 mL Schlenk flask and dissolved in 10 mL of THF, giving a violet solution. Cl-IMes (314 mg, 0.84 mmol, 2.1 equiv.) was placed in a 10 mL Schlenk tube, dissolved in 7 mL of THF and added dropwise to the solution containing $[NBu_4][OsNCl_4]$. The violet solution quickly darkened to a reddish-brown color and was stirred for 16 h at rt. The solvent was removed under high vacuum after which toluene was added. The toluene solution was filtered and the solvent was removed under high vacuum. The solid was washed with *n*-pentane (5 × 1 mL) to obtain $[OsN(Cl)_3(Cl\text{-}IMes)_2]$ (**1**) (317 mg, 0.3 mmol, **75%**) as a red solid.

^{1}H NMR (401 MHz, C_6D_6, rt) δ [ppm] = 6.52 (s, 8H, H_{Ar}), 2.24 (s, 24H, $H_{Bn,\ ortho}$), 2.05 (s, 12H, $H_{Bn,\ para}$). **^{13}C NMR** (151 MHz, C_6D_6, rt) δ [ppm] = 157.9 (s), 139.0 (s), 137.0 (s), 134.3 (s), 129.2 (s), 120.4 (s), 21.3 (s), 18.9 (s). **FT-IR** (ATR) ν [cm^{-1}]: 2960 (w), 2918 (w), 2872 (w), 1672 (w), 1615 (w), 1478 (m), 1381 (w), 1350 (w), 1289 (w), 1260 (s), 1180 (w), 1089 (br, s), 1016 (br, s), 848 (m), 797 (s), 712 (m), 661 (m), 626 (m), 573 (m). **HRMS** (ESI-TOF, positive) *m*/*z* for $[Os(N)(Cl)_2(Cl\text{-}IMes)_2]^+$ calculated: 1022.1313; measured: 1022.1301.

Synthesis of $[OsN(N_3)_3(Cl\text{-}IMes)_2]$ (2)

$[OsN(Cl)_3(Cl\text{-}IMes)_2]$ (**1**) (75.0 mg, 79.3 μmol, 1.0 equiv.) was placed in a 10 mL Schlenk tube and dissolved in 5 mL of THF. NaN_3 (20.0 mg, 308 μmol, excess) was added as a solid and the resulting suspension was stirred for 16 h at rt. The solvent was removed under high vacuum after which the residue was suspended in toluene and filtered. The solvent was removed under high vacuum and the residue was washed with *n*-pentane (3 × 1 mL) to obtain $[OsN(N_3)_3(Cl\text{-}IMes)_2]$ (**2**) (85.1 mg, 79.3 μmol, **quant.**) as a red solid.

It should be noted that azides are highly toxic and potentially explosive compounds. Although $[OsN(N_3)_3(Cl\text{-}IMes)_2]$ (2) showed no indication of explosive behavior, it should nevertheless be handled with appropriate caution.

^{1}H NMR (401 MHz, C_6D_6, rt) δ [ppm] = 6.73 (s, 8H, H_{Ar}), 2.17 (s, 24H, $H_{Bn,\ ortho}$), 2.09 (s, 12H, $H_{Bn,\ para}$). **FT-IR** (ATR) ν [cm^{-1}]: 2961 (w), 2918 (w), 2861 (w), 2816 (w), 2360 (w), 2090 (m), 2049 (br, s), 1718 (w), 1655 (w), 1604 (w), 1462 (m), 1356 (m), 1293 (m), 1262 (m), 1179 (w), 1133 (w), 1088 (m), 1037 (s), 927 (m), 849 (m), 811 (m), 739 (m), 713 (m), 688 (m), 627 (m), 542 (m). **HRMS** (ESI-TOF, positive) *m*/*z* for $[Os(N)(N_3)_2(Cl\text{-}IMes)_2]^+$ calculated: 1036.2121; measured: 1036.2072. $[Os(N)_2(N_3)(Cl\text{-}IMes)_2]^+$ calculated: 1007.1996; measured: 1007.1992.

Synthesis of $[OsN(Cl)_2(F)(Cl\text{-}IMes)_2]$ (3)

$[OsN(Cl)_3(Cl\text{-}IMes)_2]$ (**1**) (75.0 mg, 79.3 μmol, 1.0 equiv.) was placed in a 10 mL Schlenk tube and dissolved in 5 mL of THF. TlF (50.0 mg, 308 μmol, excess) was added as a solid and the resulting suspension was stirred for 16 h at rt. The solvent was removed under high vacuum after which the residue was suspended in toluene and filtered. The solvent was removed under high vacuum and the residue was washed with *n*-pentane (3 × 1 mL) to obtain $[OsN(Cl)_2(F)(Cl\text{-}IMes)_2]$ (**3**) (82.4 mg, 79.3 μmol, **quant.**) as a yellow solid.

^{1}H NMR (401 MHz, C_6D_6, rt) δ [ppm] = 6.61 (s, 8H, H_{Ar}), 2.25 (s, 24H, $H_{Bn,\ ortho}$), 2.18 (s, 12H, $H_{Bn,\ para}$). **^{19}F NMR** (377 MHz, C_6D_6, rt) δ [ppm] = −234.8 (s, 1F). **FT-IR** (ATR) ν [cm^{-1}]: 2962 (w), 2919 (w), 1601 (w), 1482 (w), 1361 (w), 1312 (w), 1259 (s), 1191 (w), 1069 (s), 1015 (s), 846 (m), 795 (s), 718 (m), 662 (m), 631 (m), 571 (m). **HRMS** (ESI-TOF, positive) *m*/*z* for $[Os(N)(Cl)(F)(Cl\text{-}IMes)_2]^+$ calculated: 1004.1579; measured: 1004.1558.

Synthesis of $[OsN(F)_3(Cl\text{-}IMes)_2]$ (4)

$[OsN(Cl)_3(Cl\text{-}IMes)_2]$ (**1**) (75.0 mg, 79.3 μmol, 1.0 equiv.) was placed in a 10 mL Schlenk tube and dissolved in 5 mL of THF. AgF (60.0 mg, 473 μmol, excess) was added as a solid and the

Open Access Article. Published on 26 February 2026. Downloaded on 3/19/2026 8:38:46 PM.
This article is licensed under a Creative Commons Attribution 3.0 Unported Licence.

resulting suspension was stirred for 16 h at rt. The solvent was removed under high vacuum after which the residue was suspended in toluene and filtered. The solvent was removed under high vacuum and the residue was washed with *n*-pentane (3 × 1 mL) to obtain $[OsN(F)_3(Cl\text{-}IMes)_2]$ (**4**) (79.9 mg, 79.3 μmol, **quant.**) as a yellow solid.

It should be noted that the success of this reaction is highly sensitive to the quality of AgF. Fresh AgF is orange in color, whereas decomposition or impurities result in a brownish appearance. The reagent should also be finely powdered to ensure completion of the reaction within 16 h. Reactions conducted with impure or coarse AgF may require extended reaction times. Sonication prior to stirring, or the use of a larger excess of AgF, can mitigate these issues.

^{1}H NMR (401 MHz, C_6D_6, rt) δ [ppm] = 6.69 (s, 8H, H_{Ar}), 2.23 (s, 24H, $H_{Bn,\ ortho}$), 2.11 (s, 12H, $H_{Bn,\ para}$). **^{19}F NMR** (377 MHz, C_6D_6, rt) δ [ppm] = −214.6 (t, ^2J = 103.7 Hz, 1F), −337.2 (d, ^2J = 103.9 Hz, 2F). **FT-IR** (ATR) ν [cm^{-1}]: 2962 (w), 2920 (w), 2861 (w), 1718 (w), 1668 (w), 1598 (w), 1482 (m), 1441 (w), 1368 (m), 1316 (w), 1260 (m), 1087 (m), 1015 (s), 850 (m), 796 (s), 696 (m), 631 (m), 583 (m). **HRMS** (ESI-TOF, positive) *m*/*z* for $[Os(N)(F)_2(Cl\text{-}IMes)_2]^+$ calculated: 988.1934; measured: 988.1933.

Author contributions

J. P. performed the synthetic work, quantum chemical calculations and formal data analysis. R. S. and T.-N. S. collected the XRD data. J. P. wrote and revised the manuscript. M. M conceptualized, coordinated and supervised the project.

Conflicts of interest

There are no conflicts to declare.

Data availability

The data supporting this study have been included as part of the supplementary information (SI). Supplementary information: general conditions; copies of NMR spectra; crystallographic data and DFT calculations. See DOI: https://doi.org/10.1039/d6dt00234j.

Data supporting this study are also available on request.

CCDC 2526370–2526373 contain the supplementary crystallographic data for this paper.[41a–d]

Acknowledgements

This work was supported by Deutsche Forschungsgemeinschaft (DFG)—Project 387284271—SFB 1349. Computing time was made available by High-Performance Computing at ZEDAT/FU Berlin. The authors acknowledge the assistance of the Core Facility BioSupraMol supported by the DFG. R. S. thanks the Fonds of the Chemical Industry (FCI) for a Kekulé Ph.D. fellowship.

References

1 A. J. Arduengo III, R. L. Harlow and M. Kline, *J. Am. Chem. Soc.*, 1991, **113**, 361–363.
2 M. N. Hopkinson, C. Richter, M. Schedler and F. Glorius, *Nature*, 2014, **510**, 485–496.
3 G. G. Zámbó, J. F. Schlagintweit, R. M. Reich and F. E. Kühn, *Catal. Sci. Technol.*, 2022, **12**, 4940–4961.
4 S. J. Hock, L.-A. Schaper, W. A. Herrmann and F. E. Kühn, *Chem. Soc. Rev.*, 2013, **42**, 5073–5089.
5 M. Jalal, B. Hammouti, R. Touzani, A. Aouniti and I. Ozdemir, *Mater. Today: Proc.*, 2020, **31**, 122–129.
6 L.-H. Chung, S.-C. Chan, W.-C. Lee and C.-Y. Wong, *Inorg. Chem.*, 2012, **51**, 8693–8703.
7 H. M. Lee, D. C. Smith, Z. He, E. D. Stevens, C. S. Yi and S. P. Nolan, *Organometallics*, 2001, **20**, 794–797.
8 U. L. Dharmasena, H. M. Foucault, E. N. dos Santos, D. E. Fogg and S. P. Nolan, *Organometallics*, 2005, **24**, 1056–1058.
9 M. Scholl, T. M. Trnka, J. P. Morgan and R. H. Grubbs, *Tetrahedron Lett.*, 1999, **40**, 2247–2250.
10 M. M. Rogers and S. S. Stahl, *N-Heterocyclic Carbenes in Transition Metal Catalysis*, Springer, Berlin, Heidelberg, 2007, pp. 21–46.
11 A. Fürstner, O. R. Thiel, L. Ackermann, H.-J. Schanz and S. P. Nolan, *J. Org. Chem.*, 2000, **65**, 2204–2207.
12 D. Jantke, M. Cokoja, A. Pöthig, W. A. Herrmann and F. E. Kühn, *Organometallics*, 2013, **32**, 741–744.
13 K. R. Jain, W. A. Herrmann and F. E. Kuhn, *Curr. Org. Chem.*, 2008, **12**, 1468–1478.
14 W. A. Herrmann, G. M. Lobmaier and M. Elison, *J. Organomet. Chem.*, 1996, **520**, 231–234.
15 C. D. Abernethy, G. M. Codd, M. D. Spicer and M. K. Taylor, *J. Am. Chem. Soc.*, 2003, **125**, 1128–1129.
16 H. Braband, T. I. Kückmann and U. Abram, *J. Organomet. Chem.*, 2005, **690**, 5421–5429.
17 R. Castarlenas, M. A. Esteruelas and E. Oñate, *Organometallics*, 2007, **26**, 2129–2132.
18 M. L. Buil, M. A. Esteruelas, I. Fernández, S. Izquierdo and E. Oñate, *Organometallics*, 2013, **32**, 2744–2752.
19 M. L. Buil, V. Cadierno, M. A. Esteruelas, J. Gimeno, J. Herrero, S. Izquierdo and E. Oñate, *Organometallics*, 2012, **31**, 6861–6867.
20 P. L. Arnold and S. Pearson, *Coord. Chem. Rev.*, 2007, **251**, 596–609.
21 C. E. Cooke, M. C. Jennings, M. J. Katz, R. K. Pomeroy and J. A. C. Clyburne, *Organometallics*, 2008, **27**, 5777–5799.
22 D. Florio, A. Annunziata, V. Panzetta, P. A. Netti, F. Ruffo and D. Marasco, *Inorg. Chem.*, 2025, **64**, 3335–3345.
23 R. G. Alabau, B. Eguillor, J. Esler, M. A. Esteruelas, M. Oliván, E. Oñate, J.-Y. Tsai and C. Xia, *Organometallics*, 2014, **33**, 5582–5596.

Open Access Article. Published on 26 February 2026. Downloaded on 3/19/2026 8:38:46 PM.
This article is licensed under a Creative Commons Attribution 3.0 Unported Licence.

24 N. Lalaoui, B. Reuillard, C. Philouze, M. Holzinger, S. Cosnier and A. Le Goff, *Organometallics*, 2016, **35**, 2987–2992.
25 T. Bolaño, M. A. Esteruelas, M. P. Gay, E. Oñate, I. M. Pastor and M. Yus, *Organometallics*, 2015, **34**, 3902–3908.
26 C.-Y. Wong, L.-M. Lai, P.-K. Pat and L.-H. Chung, *Organometallics*, 2010, **29**, 2533–2539.
27 C.-M. Che, M. H.-W. Lam and T. C. W. Mak, *J. Chem. Soc., Chem. Commun.*, 1989, 1529–1531.
28 S. M. Borisov, A. Alemayehu and A. Ghosh, *J. Mater. Chem. C*, 2016, **4**, 5822–5828.
29 Y.-Z. Lu, L.-X. Wang, R.-Y. Qi, J. Xiang, J.-Y. Liu and T.-C. Lau, *Inorg. Chem. Front.*, 2025, **12**, 3157–3165.
30 L. Raju and E. Rajkumar, *Photochemistry and Photophysics of Coordination Compounds*, Elsevier, Amsterdam, 2023, pp. 135–203.
31 C.-F. Leung, T.-W. Wong, T.-C. Lau and W.-T. Wong, *Eur. J. Inorg. Chem.*, 2005, **2005**, 773–778.
32 T. W. Wong, T. C. Lau and W. T. Wong, *Inorg. Chem.*, 1999, **38**, 6181–6186.
33 G.-S. Fang, J.-S. Huang, N. Zhu and C.-M. Che, *Eur. J. Inorg. Chem.*, 2004, **2004**, 1341–1348.
34 C. A. Urbina-Blanco, X. Bantreil, H. Clavier, A. M. Z. Slawin and S. P. Nolan, *Beilstein J. Org. Chem.*, 2010, **6**, 1120–1126.
35 K. Lott and M. Symons, *J. Chem. Soc.*, 1960, 973–976.
36 A. J. Arduengo, F. Davidson, H. V. R. Dias, J. R. Goerlich, D. Khasnis, W. J. Marshall and T. K. Prakasha, *J. Am. Chem. Soc.*, 1997, **119**, 12742–12749.
37 J. Parche, R. Sievers, T.-N. Streit and M. Malischewski, *Eur. J. Inorg. Chem.*, 2025, **28**, e202500335.
38 J. Xiang, W.-L. Man, S.-M. Yiu, S.-M. Peng and T.-C. Lau, *Chem. – Eur. J.*, 2011, **17**, 13044–13051.
39 M. K. Kesharwani, B. Brauer and J. M. L. Martin, *J. Phys. Chem. A*, 2015, **119**, 1701–1714.
40 W. P. Griffith and D. Pawson, *J. Chem. Soc., Dalton Trans.*, 1973, 1315–1320.
41 (*a*) CCDC 2526370: Experimental Crystal Structure Determination, 2026, DOI: 10.5517/ccdc.csd.cc2qswt7; (*b*) CCDC 2526371: Experimental Crystal Structure Determination, 2026, DOI: 10.5517/ccdc.csd.cc2qswv8; (*c*) CCDC 2526372: Experimental Crystal Structure Determination, 2026, DOI: 10.5517/ccdc.csd.cc2qsww9; (*d*) CCDC 2526373: Experimental Crystal Structure Determination, 2026, DOI: 10.5517/ccdc.csd.cc2qswxb.